Available online at www.sciencedirect.com

ScienceDirect

Geochimica et Cosmochimica Acta 165 (2015) 249–262

Geochimica et Cosmochimica Acta

www.elsevier.com/locate/gca

Generation of isotopically and compositionally distinct water during thermochemical sulfate reduction (TSR) in carbonate reservoirs: Triassic Feixianguan Formation, Sichuan Basin, China

Lei Jiang [a,b,*], Richard H. Worden [b,*], Chunfang Cai [a]

[a] Key Laboratory of Petroleum Resources Research, Institute of Geology and Geophysics, Chinese Academy of Sciences, Beijing 100029, China
[b] Department of Earth and Ocean Sciences, School of Environmental Sciences, Liverpool University, Liverpool L69 3GP, UK

Received 6 February 2015; accepted in revised form 20 May 2015; Available online 27 May 2015

Abstract

Thermochemical sulfate reduction (TSR), the reaction of petroleum with anhydrite in reservoirs resulting in the growth of calcite and the accumulation of H_2S, has been documented in the Feixianguan Formation dolomite reservoir in the Sichuan Basin, China. Fluid inclusion salinity and homogenization temperature data have shown that TSR results in a decrease in salinity from a pre-TSR value of 25 wt.% down to 5 wt.% as a result of water created as a byproduct of progressive TSR. We have studied the isotopic character of the water that resulted from TSR in the Feixianguan Formation by analyzing the oxygen isotopes of TSR calcite and determining the oxygen isotopes of the water in equilibrium with the TSR calcite at the temperatures determined by aqueous fluid inclusion analysis. We have compared these TSR-waters to water that would have been in equilibrium with the bulk rock, also at the temperatures determined by aqueous fluid inclusion analysis. We have found that the TSR-waters are relatively depleted in oxygen isotopes (by up to 8‰ compared to what would be expected at equilibrium between the bulk rock and water) since this type of water was specifically derived from anhydrite. The generation of relatively large volumes of low salinity, low $\delta^{18}O$ water associated with advanced TSR in the Feixianguan Formation has also been reported in the Permian Khuff Formation in Abu Dhabi and from sour Devonian fields in the Western Canada Basin. This suggests that TSR-derived water may be a common phenomenon, the effects of which on mesogenetic secondary porosity and reservoir quality have previously been underappreciated.

1. INTRODUCTION

Thermochemical sulfate reduction (TSR) occurs when petroleum reacts with aqueous sulfate, derived from the dissolution of sulfate minerals (mainly anhydrite but also celestite and barite) at elevated temperatures (greater than approximately 100–140 °C for oil and greater than 140 °C for gas) (Heydari and Moore, 1989; Worden et al., 1995; Cai et al., 2004; Worden and Smalley, 2004). A general reaction can simply be written as follows:

$$\text{sulfate} + \text{petroleum} \rightarrow \text{calcite} + H_2S \pm H_2O \pm CO_2 \pm S \pm \text{altered petroleum} \quad (R1)$$

TSR leads to significant alteration of petroleum and generates a variety of reduced forms of sulfur (S and H_2S) and oxidized forms of carbon (carbonate minerals and CO_2)

* Corresponding authors at: Department of Earth and Ocean Sciences, School of Environmental Sciences, Liverpool University, Liverpool L69 3GP, UK (L. Jiang).
E-mail addresses: jary@mail.iggcas.ac.cn (L. Jiang), r.worden@liv.ac.uk (R.H. Worden).

http://dx.doi.org/10.1016/j.gca.2015.05.033
0016-7037/

as well as a combination of water, sulfides, organosulfur compounds and bitumen (Machel, 1987; Krouse et al., 1988; Heydari and Moore, 1989; Machel et al., 1995; Worden et al., 1995, 1996, 2000; Worden and Smalley, 1996; Heydari, 1997; Bildstein et al., 2001; Cai et al., 2003, 2004, 2010).

The general reaction (R1) can be written as a series of simple stoichiometric reactions for methane (R2), ethane (R3) or other alkane gases:

$$CaSO_4 + CH_4 \rightarrow CaCO_3 + H_2S + H_2O \quad (R2)$$

$$2CaSO_4 + C_2H_6 \rightarrow 2CaCO_3 + H_2S + 2H_2O + S \quad (R3)$$

It has further been suggested (Worden and Smalley, 1996; Heydari, 1997; Orr, 1977) that any elemental sulfur that results from ethane reduction further reacts, e.g. with methane or ethane (R4). Linking R3 and R4 together results in the complete oxidation of ethane by anhydrite (R5):

$$C_2H_6 + 7S + 4H_2O \rightarrow 7H_2S + 2CO_2 \quad (R4)$$

$$7CaSO_4 + 4C_2H_6 \rightarrow 7CaCO_3 + 7H_2S + 5H_2O + CO_2 \quad (R5)$$

An important characteristic of balanced reactions of the complete oxidation of methane (R2) or ethane (R5) (and all other alkanes) by sulfate is that water is apparently created by this redox process.

Many TSR-related studies have focused on gas and oil compound stable isotopes and geochemistry (Sassen and Moore, 1988; Sassen et al., 1991; Worden et al., 1995; Worden and Smalley, 1996, 2004; Manzano et al., 1997; Mankiewicz et al., 2009; Liu et al., 2013, 2014; Hosgormez et al., 2014). Some studies have focused on the carbon and sulfur isotope ratios of minerals involved in the reactions (Videtich, 1994; Machel et al., 1995; Heydari, 1997; Cai et al., 2001; Vinogradov et al., 2006a,b). Relatively few studies have focused on the rock textural evidence and the implication for the mechanism of TSR (Heydari et al., 1988; Videtich, 1994; Machel et al., 1995; Heydari, 1997; Worden et al., 2000; Jiang et al., 2015). Only three studies have thus far directly studied the effects of TSR on oxygen isotope and water (Worden et al., 1996; Alonso-Azcarate et al., 2001; Yang et al., 2001).

The Feixianguan Formation from the Sichuan Basin offers an ideal place to study the oxygen isotope characteristics of TSR due to its relatively closed diagenetic environments (Ni et al., 2012; Cai et al., 2014; Jiang et al., 2014a), and thus the oxygen isotopic values of TSR calcites can be simply related to the original oxygen isotope of limestone and their formation temperature, the influx of diagenetic fluids, water–rock interaction, and oxygen isotope effects caused by TSR. In addition, the Sr isotope values of TSR calcite lie within the range of Feixianguan seawater (Li et al., 2012; Cai et al., 2014) and these TSR calcites show salinity values higher than seawater (>3.5 wt.% NaCl) as recorded by the fluid inclusion (Jiang et al., 2014a) this precludes the possibility that meteoric water and/or younger seawater have flowed into the Feixianguan Formation, which led to a conclusion that connate early Triassic seawater derived fluids dominated the TSR diagenesis period. Thus, in this study, we will focus on the TSR diagenetic calcites in the Feixianguan Formation dolomite reservoirs in Sichuan Basin, China, in an attempt to identify the effects of TSR upon the formation water salinity as well as the oxygen isotopic value. Specifically, we have addressed the following questions:

1. How much water was locally generated by TSR?
2. What are the isotopic and geochemical characteristics of formation water associated with TSR water?
3. What are the possible roles and effects of TSR water in carbonate reservoir?

2. GEOLOGICAL SETTING

The diamond shaped Sichuan Basin is located in the east of Sichuan Province, southwest China. It is a large intracratonic basin with an area of about 230,000 km^2 (Fig. 1A). The Sichuan Basin is tectonically-bounded by the Longmenshan fold belt in the northwest, the Micangshan uplift in the north, the Dabashan fold belt in the northeast, the Hubei-Hunan-Guizhou fold belt in the southeast, and by the Emeishan-Liangshan fold belt in the southwest.

Oolitic banks were present on the margins of the Lower Triassic trough; these were intensely dolomitized and now form good-quality gas reservoirs (Fig. 1). In the study area, the Feixianguan Formation has been subdivided into four members, in stratigraphic order: T_1f^1, T_1f^2, T_1f^3 and T_1f^4, using core and wireline log data (Cai et al., 2004; Zhu et al., 2005a). The arid climate and sea level fluctuations during the early Triassic resulted in the deposition of multiple gypsum-rich layers in the Feixianguan Formation (Ma, 2008). Anhydrite beds and shales are interbedded micritic limestones in the upper part of the Feixianguan Formation; these constitute a good regional seal for the underlying T_1f carbonate reservoir (Zhao et al., 2005) (Fig. 2).

The Feixianguan Formation reached its maximum burial depth of ~7000 m in the study area between 120–170 Ma. Temperatures in the Lower Triassic reservoirs reached 100 °C at about 200 Ma, 150 °C at 175 Ma, and a maximum temperature of about 225 °C at 120 Ma before inversion started in the Cretaceous (Fig. 3). TSR occurred in the dolomite reservoirs of the Feixianguan Formation within a temperature range of 110 °C to 220 °C. TSR produced significant amounts of H_2S as well as altering the composition and stable isotopes of the hydrocarbon gases (Cai et al., 2004, 2012; Hao et al., 2008; Liu et al., 2013, 2014).

3. SAMPLES AND METHODS

More than 100 carbonate reservoir core samples were collected from Puguang, Maoba, Luojiazhai, Dukouhe sour gas fields in the lower unit of the Triassic Feixianguan Formation. Selected samples were examined as hand specimens at the time of core sampling. Seventeen samples that showed vug-filling calcite cement textures, typical of TSR calcites (Machel, 1987; Krouse

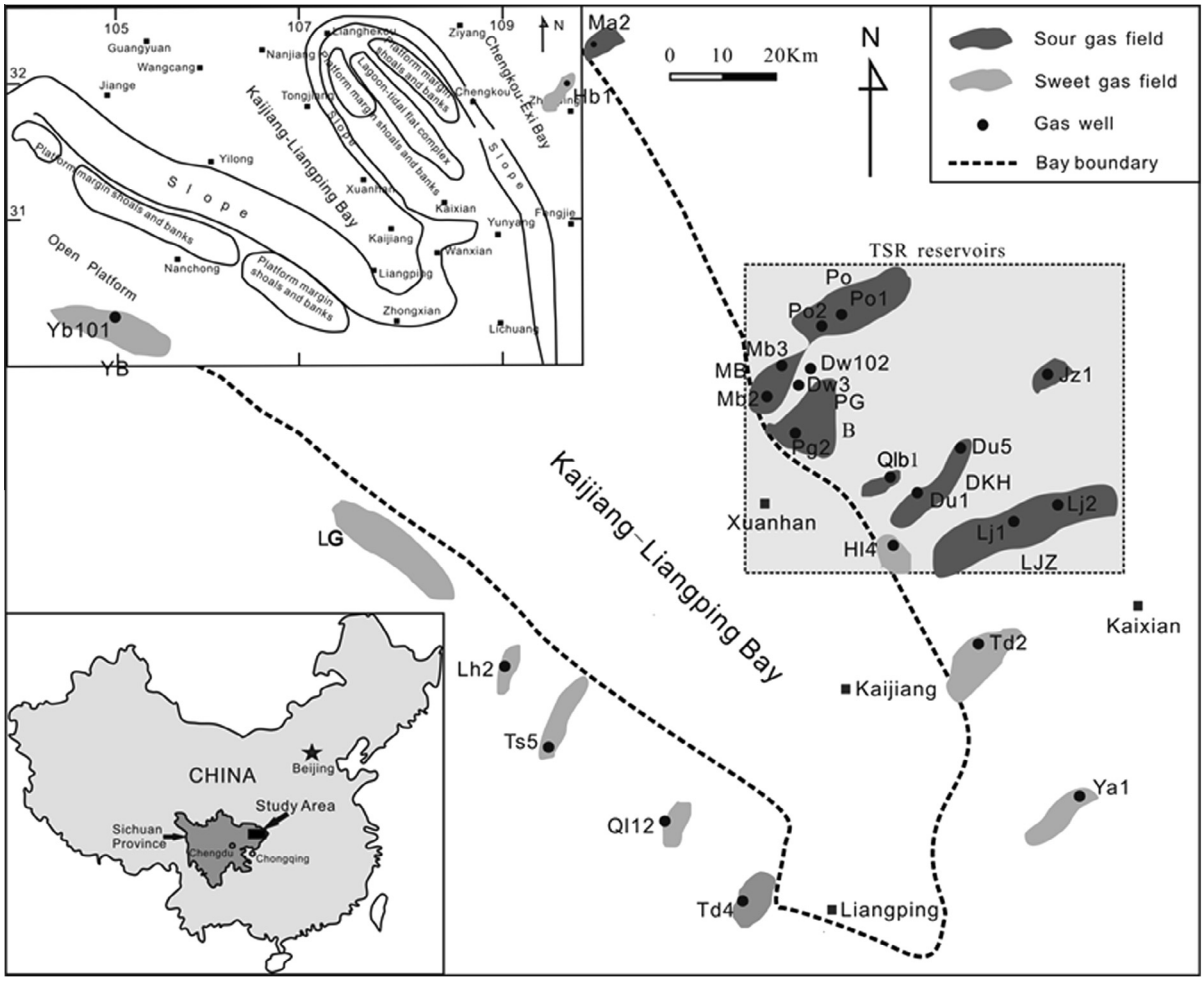

Fig. 1. Location of the study area and sampled gas fields in Feixianguan Formation reservoirs in the NE Sichuan Basin. The green rectangle area shows the area that has proven evidence of TSR (Jiang et al., 2014a).

et al., 1988; Machel et al., 1995; Worden et al., 1995, 2000; Worden and Smalley, 1996; Cai et al., 2004; Zhu et al., 2005a) were selected from the collection of core samples. All samples were petrographically studied using a standard polarizing light microscope and an SEM in backscattered electron imaging mode (BSEM) (Jiang et al., 2014a). Finely polished and etched slabs and thin sections were stained with Alizarin Red S and potassium ferricyanide to distinguish calcite from dolomite and their ferroan equivalents.

Fluid inclusions in double polished wafers were studied, using a Linkam THMSG 600/TS90 heating–cooling stage connected to Nikon petrographic microscope, to obtain thermometric data related to phase changes (liquid–vapor homogenization and last ice melting temperatures). UV fluorescence was performed on these doubly polished wafers to ascertain whether fluid inclusions were aqueous or petroleum. Inclusions were classified as being primary, or secondary (in healed fractures). Instrumental precision is ±0.1 °C. The heating and cooling process follow standard methods as applied previously to these samples (Jiang et al., 2014a). Last ice melting temperatures were converted to salinity using standard equations (Oakes et al., 1990; Bodnar, 2003).

Powdered calcite samples were extracted using a dentist's drill and subject to carbon and oxygen isotopes analyses. About 30–50 mg of drilled out sample was reacted overnight with 100% phosphoric acid at 25 °C under vacuum to release CO_2 from calcite. The CO_2 was then analyzed for carbon and oxygen isotopes on a Finnigan MAT251 mass spectrometer standardized with NBS-18. All carbon and oxygen data are reported in units per mil relative to the Vienna Peedee Belemnite (VPDB) standard. The precision for both $\delta^{13}C$ and $\delta^{18}O$ measurements is ±0.1‰.

4. RESULTS

4.1. Sedimentary environment of deposition and petrographic analysis

The Feixianguan Formation was deposited as shallow marine limestone which was dolomitized during early

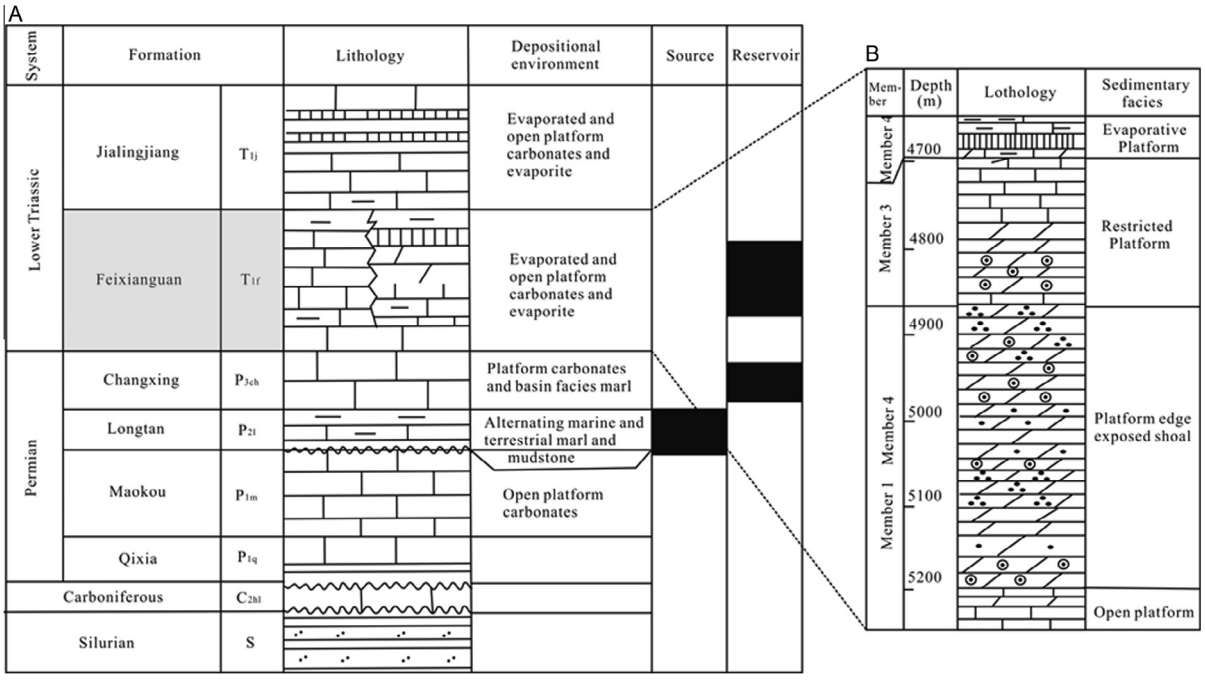

Fig. 2. Lithological column and sedimentary evolution from the Carboniferous to Triassic (A), during the early Triassic Feixianguan (B), for the NE Sichuan Basin, showing potential gas source rock and reservoirs (modified from Cai et al., 2004 and Ma et al., 2008).

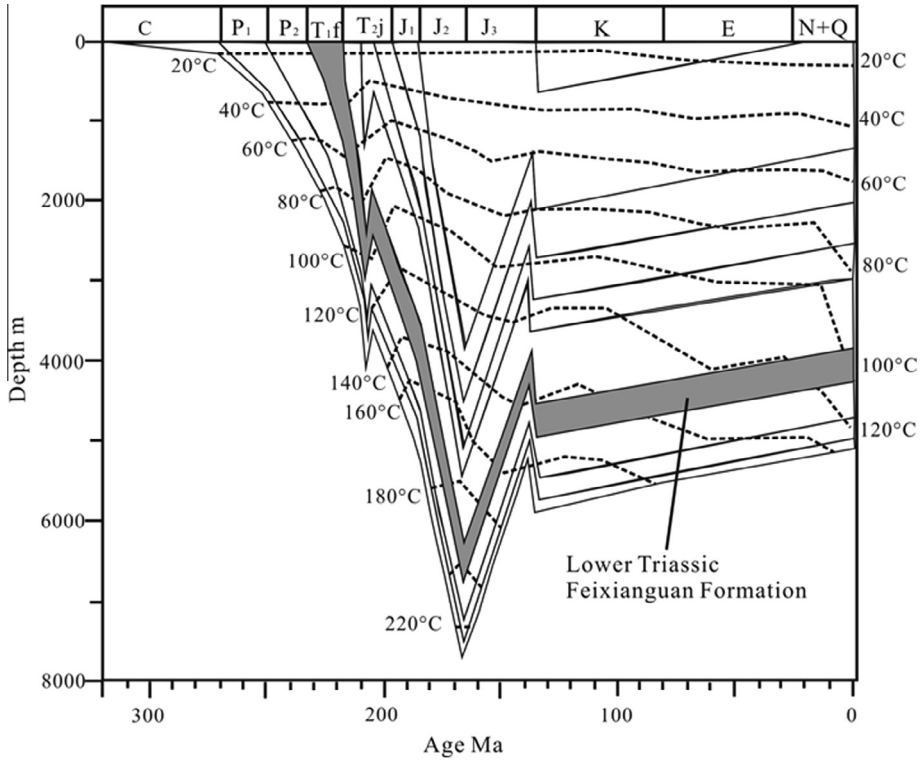

Fig. 3. Typical burial and paleo-temperature history constructed for well LJ2 from the NE part of the Sichuan Basin. Isotherms have been constrained by vitrinite reflectance and fluid inclusion measurements (modified from Cai et al., 2004).

diagenesis. The initial and main dolomitization event commenced, due to reflux processes, under near surface conditions relatively soon after deposition as shown by cement fabric and isotope evidence published previously (Jiang et al., 2013, 2014b). A subordinate later stage of dolomitization developed locally at temperatures in the range 80–140 °C as shown by petrographic, fluid inclusion, stable isotope data (Jiang et al., 2014b).

TSR-calcite (growing as a result of the oxidation of petroleum fluids by dissolved anhydrite) and non-TSR calcite cements of the Feixianguan Formation form the focus of this paper. TSR calcite in the Feixianguan reservoirs has a vug- and pore-filling texture (Fig. 4) and is totally nonluminescent under CL (Cai et al., 2004, 2014; Zhu et al., 2005a; Li et al., 2012). Two types of TSR calcite were identified in the Feixianguan Formation. The dominant type of TSR calcite sits in pores surrounding dolomite rhombs (here called poikilotopic TSR calcite) and is typically 50–200 μm in length (Fig. 4A and B). Also present, though less common, is a replacive form of TSR calcite that exists as a rind on the corroded surfaces of anhydrite nodules in dolomicrite (Zhu et al., 2005a; Jiang et al., 2014a).

Non-TSR related calcite (both pre- and post-) are present in vugs and veins. Some calcite pre-dates the final stage of dolomitization (fluid inclusion temperatures from the later dolomite homogenized at 80 to 140 °C) (Jiang et al., 2014b) and thus grew before TSR calcite. Calcite veins can easily be observed in thin-section and core (Fig. 4C and D) since they are up to several centimeters wide and have lengths >1 meter. Calcite veins cross-cut all early and late stage diagenetic cements and fabrics, including TSR calcite, showing that vein calcite post-date the growth of TSR calcite.

4.2. Fluid inclusion petrography, aqueous homogenization temperatures and salinity

Doubly-polished detachable wafers (15 in total) of both non-TSR calcite and TSR calcites were prepared from subsurface core samples from a number of wells in various dry and variably sour gas fields in the study area. Data from these samples have been supplemented by previously published fluid inclusion data from TSR and non-TSR calcite (Hao et al., 2009; Jiang et al., 2014a). Pre- and post-TSR calcite, as well as TSR-calcite, contain primary, two-phase aqueous inclusions. These fluid inclusions showed no signs of necking, deformation or leakage, and had effectively uniform liquid–vapor ratios at room temperature, suggesting that the homogenization temperature data are not an artifact of post-formational processes.

There are two type of TSR calcite; those that have oil-filled inclusions coeval with the aqueous inclusions and those that are demonstrably free of oil-inclusions (Jiang et al., 2014a). The measured aqueous fluid inclusion homogenization temperature data in TSR calcite range from about 116 °C to more than 180 °C (Figs. 5 and 6; Table 1). TSR calcite with associated oil inclusions has aqueous inclusions that homogenize at a minimum of 116 °C and a mode of homogenization temperature values between 130 and 140 °C with an absolute maximum of

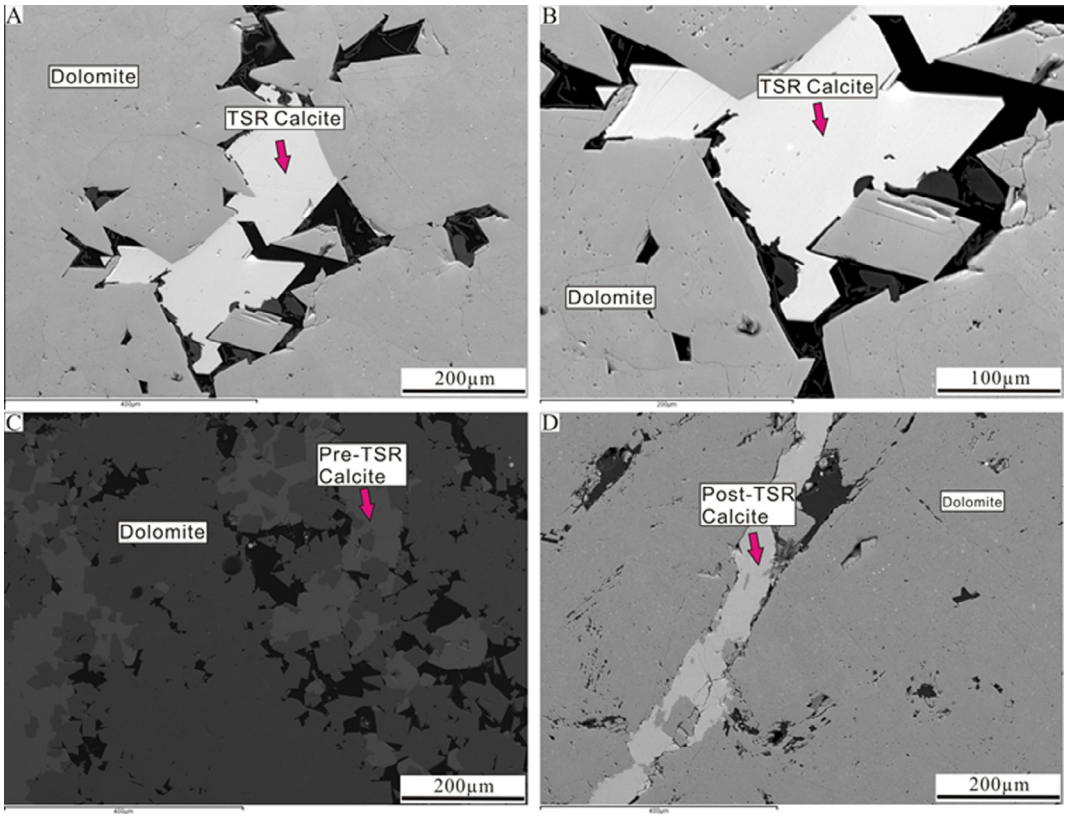

Fig. 4. Photographs showing the presence of pre-TSR, TSR, and post-TSR calcite in the Feixianguan Formation. (A) BSEM image of pore-filling TSR calcite (arrowed) in oolitic dolomite, well Du4, depth 4790.8 m. (B) BSEM image of pore-filling TSR calcite (arrowed) in oolitic dolomite, well LJ2. (C) BSEM image showing pore-filling pre-TSR calcite in dolomicrite, well JZ1, depth 2978.8 m. (D) BSEM image showing fracture-filling post-TSR calcite in dolomicrite, well DW102, depth 4820.5 m.

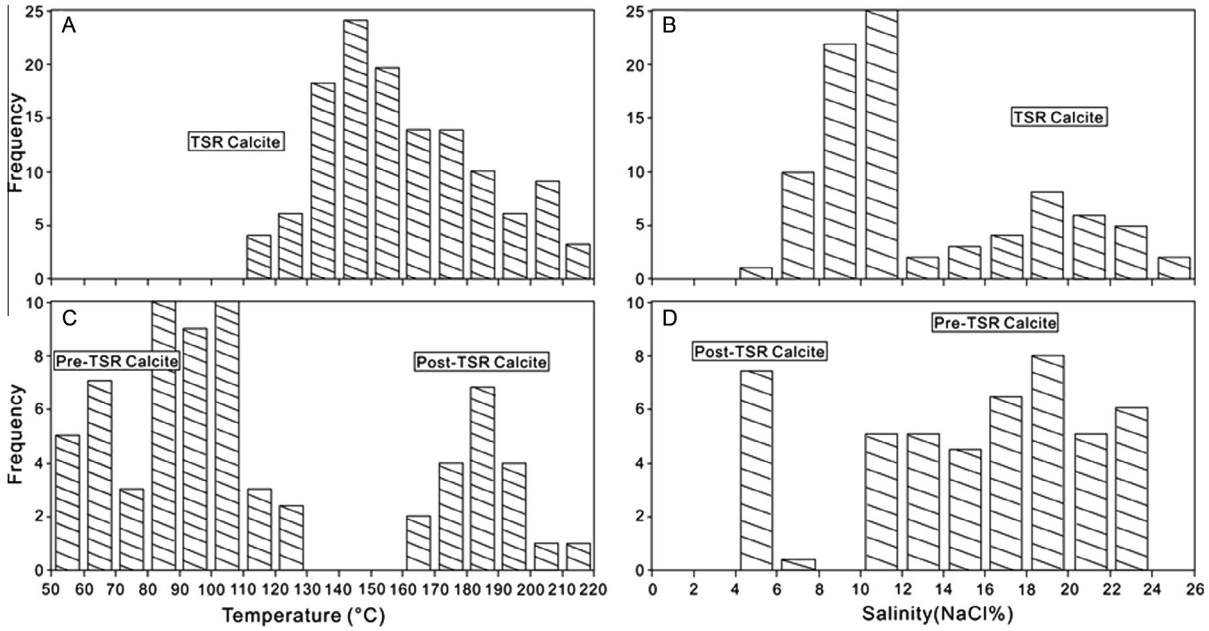

Fig. 5. Fluid inclusion data from pre-TSR calcite, TSR calcite, and post-TSR calcite in the Feixianguan Formation (including data from Jiang et al., 2014a). (A) Fluid-inclusion homogenization temperature data, and (B) salinity data from aqueous inclusions from TSR calcite. (C) Fluid-inclusion homogenization temperatures, and (D) salinity data from aqueous inclusions from pre-TSR and post-TSR calcite.

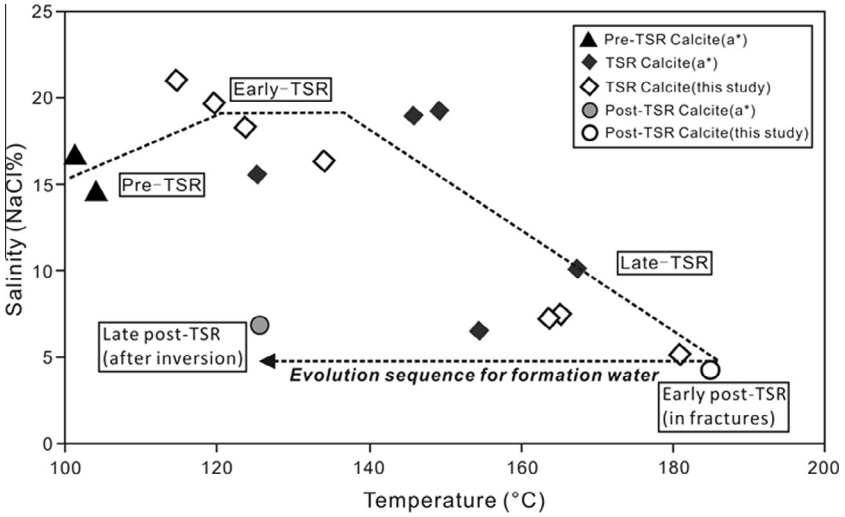

Fig. 6. Comparison of average salinity and homogenization temperature from fluid inclusions in pre-TSR, TSR, and post-TSR calcites in the Feixianguan Formation.

about 160 °C; this has been labeled oil-phase TSR (Jiang et al., 2014a). TSR calcite free of oil inclusions has aqueous inclusions that homogenize at a minimum of 135 °C and has a spread of homogenization temperatures that extends to the maximum burial temperature; this has been labeled gas-phase TSR (Jiang et al., 2014a). The salinity of the aqueous inclusions in TSR calcite varies from 5.1 to 21.0 wt.% (Figs. 5 and 6; Table 1). Salinity values seem to decrease with the increasing temperature of trapping both for the entire dataset and for individual samples. Oil-phase TSR calcite has aqueous inclusions with salinity from greater than 24 to as low as 8 wt.% with a mode at about 21 wt.%. Gas-phase TSR calcite has aqueous inclusions with salinity ranging from 19 to 5 wt.% with a mode of 10 wt.%.

Fluid inclusions from pre-TSR calcite have homogenization temperatures between 101 and 104 °C (Figs. 5 and 6). Salinity data from pre-TSR calcite range from 10 to >22 wt.%. Fluid inclusions from post-TSR calcite have homogenization temperatures between 125 and 185 °C (Figs. 5 and 6). Salinity data from post-TSR calcite range from 4.2 to 6.8 wt.% (Fig. 5; Table 1). In the Feixianguan

Table 1
Carbon and oxygen isotope, and average value of fluid inclusion salinity and homogenization temperature (Th) of diagenetic calcites from dolomite hosted reservoirs of Feixianguan Formation, Northeast Sichuan Basin: data below detection or no data available; a*: data from Jiang et al. (2014a); b*: data from Li et al. (2012); c*: data from Hao et al. (2009); d*: data from Wang et al. (2007); e*: data from Zhu et al. (2005a,b); f*: Wang et al. (2002).

Well	Depth(m)	Host mineral	$\delta^{13}C$ (‰VPDB)	$\delta^{18}O$ (‰ VPDB)	Th (°C)	Salinity (%NaCl)
JZ-1	2978.8	Pre-TSR calcite	−0.5 a*	−4.9 a*	101.1 a*	16.6 a*
LJ-1	3470.4	Pre-TSR calcite	–	–	104.0 a*	14.4 a*
PG-6	4876	TSR calcite	–	–	114.6	21
DW-102	4900.7	TSR calcite	−1.1 a*	−9.5 a*	145.8 a*	18.9 a*
LJ-6	3936	TSR calcite	–	–	149.2 a*	19.2 a*
D-5	4793	TSR calcite	−16.5 b*	−8.6 b*	167.4 a*	10.0 a*
PG-1	5421.2	TSR calcite	−10.1	−10.5	164.1	–
PG-1	5423.2	TSR calcite	−12.1	−7.8	150.6	–
PG-1	5426.5	TSR calcite	−12	−10.9	163.4	–
PG-1	5428.4	TSR calcite	−9.8	−12.3	173.5	–
PG-1	5428.6	TSR calcite	−12.6	−11.8	169.9	–
PG-2	4784.5	TSR calcite	−10	−9.2	172	–
PG-2	4775.2	TSR calcite	−8.7	−12.8	170.9	–
PG-2	4779.9	TSR calcite	–	–	180.9	5.1
PG-3	5894.4	TSR calcite	–	–	154.5 c*	6.4 c*
PG-4	5790	TSR calcite	−7.1	−12.6	171.1	–
PG-6	4862.7	TSR calcite	−5.8	−12.9	178.4	–
PG-6	5145.6	TSR calcite	−7.8	−10.8	183.4	–
PG-6	5378.4	TSR calcite	–	–	163.6	7.2
MB-3	3876	TSR calcite	−7.8	−6.3	131.2	–
LJ-6	–	TSR calcite	–	–	149.2 a*	19.2 a*
LJ-2	3400.7	TSR calcite	−16.3	−7.9	134.1	16.3
LJ-2-1	–	TSR calcite	−13.5	−8.2	165.2	7.5
LJ-7	–	TSR calcite	−18.4 d*	−6.1 d*	123.6	18.4
LJ-5	3002.9	TSR calcite	−6.1 e*	−5.7 e*	–	–
P-1	–	TSR calcite	−7.3 f*	−6.4 f*	125.2	–
P-1	3464.7	TSR calcite	−18.2 e*	−6.3 e*	–	–
P-3	3536	TSR calcite	−17.0 e*	−5.9 e*	–	–
P-4	3238	TSR calcite	−16.3 e*	−6.0 e*	119.7	19.6
PG-6	–	Post-TSR calcite	0.6 a*	−5.8 a*	125.6 a*	6.8 a*
DW-1	4735	Post-TSR calcite	1.4	−6.7	185	4.2

Formation, salinity values seem to broadly decrease with increasing temperature from pre-TSR diagenesis to post-TSR diagenesis (Figs. 5 and 6).

4.3. Stable isotope analysis

New carbon and oxygen isotope data from carbonate host rocks, TSR-calcite and pre- and post-TSR calcite (Table 1) have been supplemented by previously published data (Wang et al., 2002, 2007; Zhu et al., 2005a; Li et al., 2012). The Feixianguan Formation matrix dolomite displays a narrow range of carbon isotope values between 0‰ and 4‰ V-PDB and oxygen isotopic values between −3‰ and −7‰ V-PDB (Fig. 7). Most of the pre- and post-TSR calcite carbon isotope data lie between −0.5‰ and 2‰ V-PDB with oxygen isotope data between −6‰ and −8‰ V-PDB.

In contrast, TSR calcite has a wide range of carbon isotope values between −3‰ and −19‰ V-PDB and narrower range of oxygen isotope values between −5.7‰ to −9.5‰ V-PDB (Fig. 7). The negative carbon isotope value (Fig. 7, Table 1) confirms that there is a significant proportion of organic carbon in TSR (Worden et al., 1995; Worden and Smalley, 1996; Machel, 2001; Cai et al., 2004, 2014; Zhu et al., 2005a).

5. DISCUSSION

5.1. Water generated by TSR

Based on the detailed petrographic and gas chemistry studies, it has been unequivocally demonstrated that thermochemical sulfate reduction has occurred in the Feixianguan Formation in the Sichuan Basin (Cai et al., 2004, 2010, 2013, 2014; Zhu et al., 2005a; Hao et al., 2008; Liu et al., 2013, 2014; Jiang et al., 2014a,b). In the Feixianguan Formation, TSR has largely occurred due to gas-reduction and not oil reduction. The gas in the Feixianguan Formation varies from a dryness of 95% to 100% (CH_4/C_nH_{2n+2}) and it has been shown that at least some of the TSR is due to methane oxidation by sulfate. Reference to simple stoichiometric reactions of the total oxidation of methane (R2) or ethane (R5) by anhydrite reveals that these processes apparently generate water to correctly mass balance. Note that the TSR-created water should be low salinity since it is essentially pure H_2O.

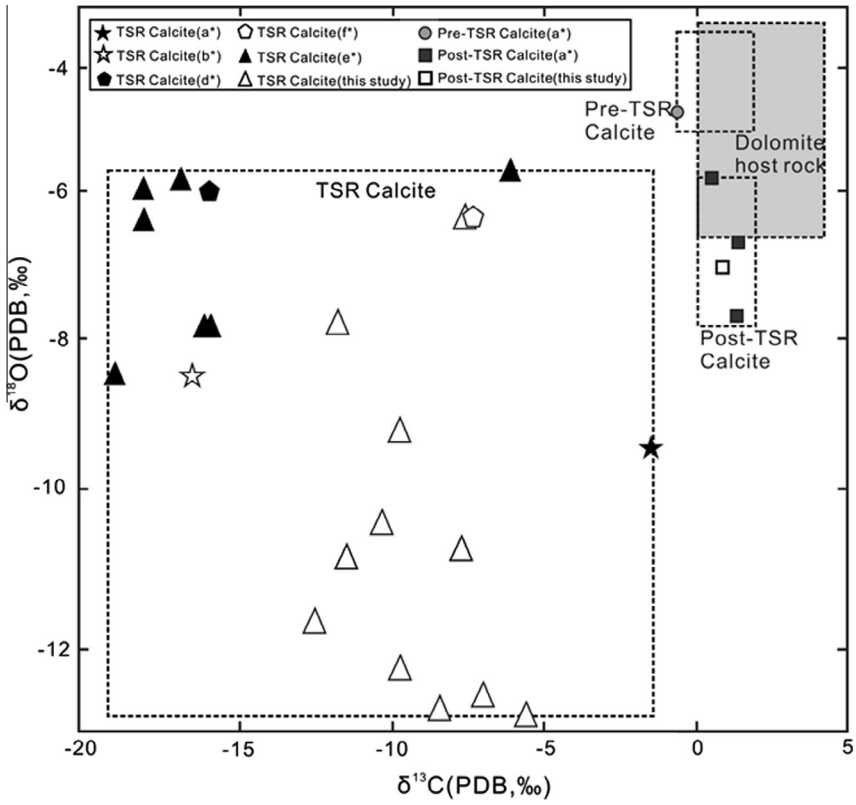

Fig. 7. The carbon and oxygen isotopic compositions of pre-TSR, TSR and post-TSR calcites in the Feixianguan Formation. The colored rectangles show the ranges of data of the different diagenetic carbonate cement phases. Previously published data (a* data from Jiang et al., 2014a; b* data from Li et al., 2012; d* data from Wang et al., 2007; e* data from Zhu et al., 2005a,b; f* Wang et al., 2002) differentiated from the new data presented here.

The first study to identify the generation of water by TSR was from the Permian Khuff Formation in Abu Dhabi (Worden et al., 1996). However, this led to some discussion since the same phenomenon was apparently not found in another sour province (Machel, 1998; Worden et al., 1998). Since then, several case studies from around the world have supported the notion of the creation of water during TSR (Yang et al., 2001; Du et al., 2007; Vandeginste et al., 2009).

In the Feixianguan Formation, the connate water was seawater, thus the initial formation water has salinity most likely being closed to 3.5 wt.% (Jiang et al., 2014b). During shallow diagenesis (25–40 °C), the Feixianguan Formation was characterized by brine reflux dolomitization (Jiang et al., 2013, 2014b). This was followed by the invasion of highly saline brine from the overlying Jialingjiang Formation, which resulted in localized burial dolomitization between 80 and 140 °C (Zhu et al., 2007; Jiang et al., 2013, 2014b). The salinity of formation water in the Feixianguan Formation was up to 25 wt.% during burial dolomitization (Jiang et al., 2014b). This high formation water salinity is also reflected in the pre-TSR calcite cement (Figs. 5 and 6) confirming that, before TSR commenced, the formation water had a salinity of up to 25 wt.%. The lower temperature, i.e. earlier, TSR calcite has high salinity fluid inclusions, presumably reflecting the pre-TSR formation water salinity (Fig. 6). However, during TSR, Feixianguan Formation water salinity decreased with progressively increasing burial temperatures reaching values as low as 5 wt.% at the highest temperatures (Fig. 6). This pattern from the Feixianguan Formation concurs with the pattern of TSR leading to reduced formation salinity reported previously (Worden et al., 1996; Yang et al., 2001; Vandeginste et al., 2009). Significantly, the lowest formation water salinity revealed by fluid inclusions from TSR calcite in the Feixianguan Formation is close to the current formation water salinity (Li et al., 2012). The reduction in salinity from 25 wt.% to as low as 5 wt.% suggests that a given volume of the original saline formation water was diluted by a factor of approximately four or more by the addition of fresh water due to the oxidation of petroleum gases during TSR (R2, R5). The relative volume of water generated by TSR in this study is similar to that reported from sour gas provinces in Abu Dhabi and in the Western Canada Sedimentary Basin (Worden et al., 1996; Yang et al., 2001).

5.2. Interpretation of oxygen isotopes of formation water based on TSR calcite data

The average temperatures of growth of TSR calcite were obtained from aqueous fluid inclusion homogenization temperatures (Table 1). The measured calcite $\delta^{18}O$ values were then used, in conjunction with the fluid inclusion

temperatures, to generate the $\delta^{18}O$ values of the formation water associated with TSR calcite growth by employing a standard calcite-water oxygen isotope fractionation equation (Friedman and O'Neil, 1977) and the aqueous fluid inclusion homogenization temperatures. The results of these calculations are presented in Table 2 and are labeled $\delta^{18}O_{TSR\text{-}water}$. Identical calculations were made for the pre- and post-TSR calcite thus revealing the $\delta^{18}O$ values of the formation water in equilibrium with pre- and post-TSR calcite (Table 2).

5.3. Interpretation of theoretical formation water oxygen isotope values based on bulk rock data

It can be assumed that the early Triassic Feixianguan limestones originally had a $\delta^{18}O$ value of about $-5‰$ VPDB after the transformation of aragonite and high-Mg calcite to low-Mg calcite (Veizer et al., 1999; Korte et al., 2005a,b; Chafetz et al., 2008; Huang et al., 2012). Another calculation was performed using the same calcite-water oxygen isotope fractionation equation to predict what the $\delta^{18}O$ values of the formation water would have been if the initial bulk marine limestone (with the $\delta^{18}O$ value of about $-5‰$ VPDB) had simply re-equilibrated with formation water (i.e. no TSR effect) at the temperature defined by aqueous fluid inclusions. This modeled output is labeled $\delta^{18}O_{BR\text{-}water}$ (where BR-water stands for bulk rock water).

5.4. Prediction of the oxygen isotopes of water derived from the reduction of anhydrite

The oxygen in TSR calcite is derived from anhydrite and thus the oxygen isotopes of TSR calcite must be influenced by the oxygen isotopes of the parent anhydrite. However, up to this time, there have been no reports of $\delta^{18}O$ values from anhydrite from the Feixianguan Formation although this is not unusual since there have been rather few reports of anhydrite oxygen isotopes globally.

It has been reported previously that mineral sulfate-$\delta^{18}O$ values positively correlated with mineral sulfate-$\delta^{34}S$ value during the Triassic and other geological times (Claypool et al., 1980; Alonso-Azcarate et al., 2006; Boschetti et al., 2011). Hence, we have employed a linear relationship, based on these publications, between sulfate-$\delta^{34}S$ and sulfate-$\delta^{18}O$ ($\delta^{18}O_{Anhydrite} = 1.146 \times \delta^{34}S_{Anhydrite} - 4.3194$, $R^2 = 0.4856$) to predict the oxygen isotope signature of Feixianguan Formation anhydrite in the Sichuan Basin. An average $\delta^{34}S$ value of 21.92‰ CDT was calculated for the Feixianguan Formation anhydrite ($n = 16$) (Zhu et al., 2005a) thus suggesting that the Feixianguan Formation anhydrite $\delta^{18}O$ value was 20.81‰ V-SMOW.

The theoretical $\delta^{18}O$ of water that would result from the TSR-induced breakdown of anhydrite to calcite and water was calculated by using the derived anhydrite $\delta^{18}O$ value of 20.81‰ V-SMOW, a published calcite-water fractionation equation (Friedman and O'Neil, 1977) and the recognition that the four oxygen atoms in anhydrite split with three going to calcite and one into the water (Worden et al., 1996). The results of this calculation (labeled $\delta^{18}O_{AB\text{-}water}$, where AB-water represents water due to anhydrite TSR breakdown) are presented in Table 2 and were derived using the following equation:

$$\delta^{18}O_{AB-water} = 3/4 \times [(2.78 \times 10^6/T^2) - 2.89] \quad (1)$$

For reference, the calcite that should theoretically result from the breakdown of anhydrite during TSR (labeled $\delta^{18}O_{AB\text{-}calcite}$) can be derived with the matching equation:

$$\delta^{18}O_{AB-calcite} = 1/4 \times [(2.78 \times 10^6/T^2) - 2.89] \quad (2)$$

This approach assumes that TSR occurred predominantly at the mean temperature recorded by fluid inclusions in TSR calcite. It also assumes there was no kinetic isotope fractionation of oxygen isotopes during TSR (i.e. assuming that TSR was a bulk process with no preferential reaction of ^{16}O-anhydrite).

5.5. Comparison of TSR-water and bulk rock water

The water that was associated with growth of TSR calcite ($\delta^{18}O_{TSR\text{-}water}$) can be compared to the theoretically modeled water that would have been in simple isotopic equilibrium with the host rock ($\delta^{18}O_{BR\text{-}water}$) (Table 2). The $\delta^{18}O_{TSR\text{-}water}$ values are considerably lighter than the $\delta^{18}O_{BR\text{-}water}$ values throughout the data set. This suggests that the water that resulted from TSR was isotopically-distinct from any formation water that was in equilibrium with the bulk rock before TSR started.

The difference between $\delta^{18}O_{TSR\text{-}water}$ and $\delta^{18}O_{BR\text{-}water}$ has been calculated and is labeled $\Delta\delta^{18}O$ (Table 2). $\Delta\delta^{18}O$ varies from $-1‰$ to $-8‰$ showing that there was a considerable deviation from the water that would be expected from simple isotopic equilibrium with the host rock. $\Delta\delta^{18}O$ has been plotted as a function of fluid inclusion homogenization temperature (Fig. 8). The water in equilibrium with the pre-TSR calcite is effectively the same as that expected for the bulk rock calculation (Table 2) and this value has been added to Fig. 8. The water in equilibrium with the post-TSR calcite is $-0.8‰$ (Table 2) and so is only marginally different to that expected from the bulk rock calculation, this value has also been added to Fig. 8.

Before TSR, there is negligible difference between the determined water-$\delta^{18}O$ from the pre-TSR calcite $\delta^{18}O$ and $\delta^{18}O_{BR\text{-}water}$; the difference between $\delta^{18}O_{TSR\text{-}water}$ and $\delta^{18}O_{BR\text{-}water}$ ($\Delta\delta^{18}O$) varies with temperature, and thus the degree or extent of TSR. The maximum difference occurs at the highest temperature (Fig. 8). Following TSR, as recorded in the post-TSR calcite, there is negligible difference between the determined water-$\delta^{18}O$ from the post-TSR calcite $\delta^{18}O$ and modeled $\delta^{18}O_{BR\text{-}water}$. This suggests that the effect of the addition of TSR water ceased once TSR has terminated. There appears to be a cycle of progressively and increasingly affected formation water $\delta^{18}O$ during TSR which then stops as soon as TSR stops (Fig. 8).

Note that there are no alternative plausible sources of isotopically-light (and low salinity) water that could have influenced the deeply buried and gas-charged Feixianguan Formation in the way shown (Figs 5–8). Gas-filled formations have negligible relative permeability for water

Table 2
Model $\delta^{18}O$ values of water and calcite. Where TSR-water is the water that is interpreted to be in equilibrium with TSR-calcite at the temperature of growth, BR-water is the water interpreted to be in equilibrium with the host bulk rock at the equivalent temperature of TSR calcite growth.

Sample no.	Diagenetic stage	Th (°C) Measured from fluid inclusion	Measured calcite $\delta^{18}O$ ‰ VPDB	Measured calcite $\delta^{18}O$ ‰ V-SMOW	Derived $\delta^{18}O_{TSR\text{-}water}$ ‰ SMOW based on measured calcite $\delta^{18}O$ at Th (°C)	Model formation water $\delta^{18}O_{AB\text{-}water}$ ‰ SMOW assuming breakdown of anhydrite $\delta^{18}O$ of 20.81 at Th (°C)	Model $\delta^{18}O_{BR\text{-}water}$ ‰ SMOW based on equilibration of bulk marine limestone at Th (°C)	$\Delta\delta^{18}O$ ‰ SMOW $\delta^{18}O_{TSR\text{-}water} - \delta^{18}O_{BR\text{-}water}$
JZ-1	Pre-TSR	101.1	−4.9	25.9	8.89	8.08	8.79	0.10
P-4	TSR	119.7	−6.0	24.7	9.60	9.46	10.63	−1.03
LJ-7	TSR	123.6	−6.1	24.6	9.85	9.72	10.98	−1.13
P-1	TSR	125.2	−6.4	24.3	9.68	9.83	11.12	−1.44
LJ-2	TSR	134.1	−7.9	22.8	8.89	10.40	11.88	−2.99
DW-102	TSR	145.8	−9.5	21.1	8.17	11.09	12.81	−4.64
LJ-2-1	TSR	165.2	−8.2	22.5	10.88	12.12	14.18	−3.30
D-5	TSR	167.4	−8.6	22.1	10.61	12.23	14.32	−3.71
PG-1	TSR	164.1	−10.5	20.1	8.46	12.06	14.10	−5.65
PG-1	TSR	150.6	−7.8	22.9	10.24	11.36	13.16	−2.93
PG-1	TSR	163.4	−10.9	19.7	8.02	12.03	14.06	−6.04
PG-1	TSR	173.5	−12.3	18.2	7.21	12.52	14.71	−7.50
PG-1	TSR	169.9	−11.8	18.8	7.43	12.35	14.48	−7.06
PG-2	TSR	172.0	−9.2	21.4	10.25	12.45	14.62	−4.37
PG-2	TSR	170.9	−12.8	17.7	6.52	12.40	14.55	−8.03
PG-4	TSR	171.1	−12.6	17.9	6.70	12.41	14.56	−7.86
PG-6	TSR	178.4	−12.9	17.6	6.85	12.74	15.01	−8.17
PG-6	TSR	183.4	−10.8	19.8	9.31	12.97	15.31	−6.00
MB-3	TSR	131.2	−6.3	24.4	10.31	10.22	11.64	−1.33
DW-1	Post-TSR	185.0	−6.7	24.0	13.65	13.04	15.40	−1.75
PG-6	Post-TSR	125.6	−5.8	24.9	10.33	9.85	11.16	−0.82

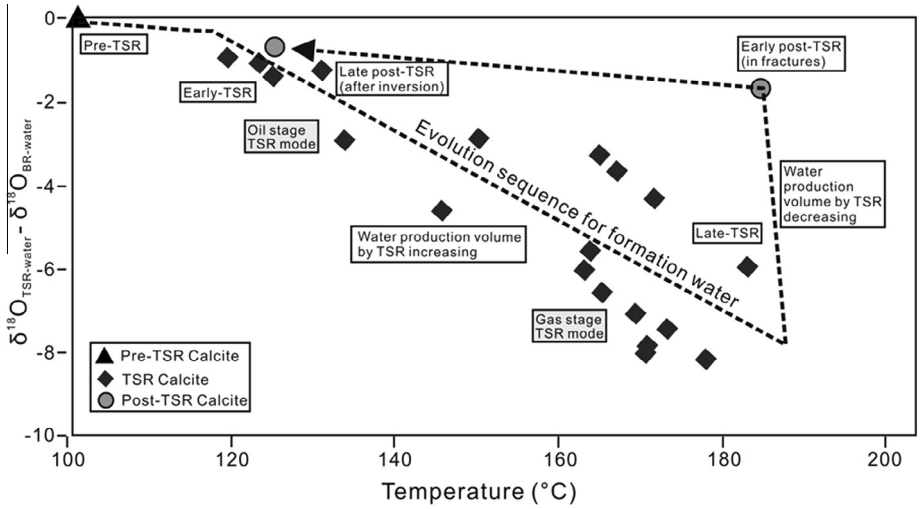

Fig. 8. The relationship between temperature and the deviation of TSR-related water from the expected formation water $\delta^{18}O$ assuming water equilibration with Lower Triassic marine calcite at increasing temperature ($\Delta\delta^{18}O$ value; equal to $\delta^{18}O_{TSR\text{-}water} - \delta^{18}O_{BR\text{-}water}$). Data have been differentiated for pre-TSR calcite, TSR calcite, and post-TSR calcite in the Lower Triassic Feixianguan Formation. The figure shows that isotopically-distinct (low $\delta^{18}O$) water was produced during TSR.

(Archer and Wall, 1986) implying that any mass influx of flowing water, from any source, is highly unlikely. Also, there are no indications of meteoric water influx or any other source of low salinity, isotopically light water from petrological, trace and rare earth elements (REE), Sr isotopes, or carbon and oxygen isotopes of other diagenetic minerals (Cai et al., 2004, 2014; Zhu et al., 2005b; Li et al., 2012; Jiang et al., 2013; Jiang et al., 2014a,b).

It is significant that this pattern of relative reduction of formation water $\delta^{18}O$ was also found in the TSR-affected Khuff Formation (Worden et al., 1996) where the formation water $\delta^{18}O$ decreased from about 8‰ to about 2‰ SMOW as TSR proceeded.

5.6. Cause of the isotopically-light TSR water in the Feixianguan Formation

Water associated with TSR in the Feixianguan Formation has relatively low $\delta^{18}O$ values ranging from 6.5‰ to 10.9‰ ($\delta^{18}O_{TSR\text{-}water}$, Table 2). The water that theoretically results from TSR breakdown of anhydrite at each specific temperature, assuming that initial anhydrite had a $\delta^{18}O$ of 20.8‰ and assuming no kinetic isotope effect, ranges from 9.5‰ to 13.0‰ SMOW ($\delta^{18}O_{AB\text{-}water}$, Table 2). The calculated TSR-water thus seems to have lower $\delta^{18}O$ values than what should have been produced by anhydrite breakdown given the assumption employed.

The pre-TSR anhydrite $\delta^{18}O$ value of 20.8‰ is no more than an estimate (see previous). It is possible that this value is an overestimate. It is also not necessarily safe to assume that TSR occurred by a bulk reaction (anhydrite dissolved and then totally reacted with petroleum phases). It is possible that there was a kinetic isotope effect during TSR: the ^{16}O-fraction of anhydrite dissolved or reacted more quickly than the ^{18}O fraction of anhydrite thus resulting in lower initial $\delta^{18}O$ values for the (early) reaction products. It is possible that a combination of these factors can explain why the calculated $\delta^{18}O_{TSR\text{-}water}$ values are lower than the estimated $\delta^{18}O_{AB\text{-}water}$ values (Table 2).

5.7. Implications of TSR water and its oxygen isotope fraction

Water recorded in aqueous fluid inclusions following TSR from Sichuan Basin (data reported here), from Abu Dhabi (Worden et al., 1996), and from the Western Canada Basin (Yang et al., 2001), have diluted the previously saline formation from initial high values (~25 wt.%) to low values (~5 wt.%). It can be surmised that the added water had very low salinity. Based on reactions R2 and R5, the newly created water should have zero salinity.

The newly created water tends to have relatively lower $\delta^{18}O$ values than the ambient formation water (interpreted from mineral $\delta^{18}O$ values). In the Permian Khuff Formation in Abu Dhabi, water interpreted to be present when TSR was most intense had a $\delta^{18}O$ of about 1‰ or 2‰ in contrast to water at early stage TSR that had a $\delta^{18}O$ of up to 10‰ (Worden et al., 1996). In the Triassic Feixianguan Formation reported here, water interpreted to be present when TSR was most intense had a $\delta^{18}O$ of about 6.5‰ in contrast to the water that would have been present had TSR not occurred (labeled bulk-rock water; Table 2) that would have a $\delta^{18}O$ of up to 14.5‰. The oxygen isotope difference (minimum to maximum TSR effect) is similar for both the Permian Khuff Formation and the Triassic Feixianguan Formation.

The generation of significant volumes of water by TSR is overlooked at peril (Worden et al., 1996) since the added water can have a range of consequences including a TSR-autocatalytic effect (since the TSR reaction happens between dissolved sulfate and petroleum; more water represents more opportunity for reaction); influences on rock properties recorded by resistivity and other logs (in rocks actively undergoing TSR); and ongoing diagenetic

alteration of the rock mediated by the increased amount of water as a result of TSR. Note that we have not necessarily identified formation-wide dilution of saline pore water by low $\delta^{18}O$ water in the Feixianguan Formation in this study; rather we have identified dilution at the sites at which TSR has occurred and at which the resulting calcite grew.

Interestingly, the deeply buried (up to 5000 m) Feixianguan Formation dolomite reservoirs with high H_2S concentrations (average value at about 15%), show anomalously high porosity (up to 15%). At least some of the high porosity has been proposed to be the result of late stage dissolution and is thus secondary porosity; this dissolution has been linked to TSR (Ma et al., 2008; Zhao et al., 2011; Cai et al., 2014). The dilution of pre-existing formation water by up to four times (by volume) with new water resulting from TSR may lead to insights into naturally elevated carbonate reservoir quality during deep burial environments (Ehrenberg et al., 2012). The generation of H_2S by TSR may lead to the development of acidic fluids that could locally dissolve carbonate minerals in the reservoir (Worden et al., 1996; Cai et al., 2014). The newly created water that is added to the carbonate reservoir systems due to TSR, as well as the associated H_2S generated by TSR, could lead to the dissolution of minerals and creation of secondary porosity deep in sedimentary basins. This has clear and significant implications for petroleum exploration deep in sedimentary basins (Heydari and Moore, 1989; Worden et al., 1996; Heydari, 1997; Ehrenberg et al., 2012; Cai et al., 2014).

6. CONCLUSIONS

1. TSR calcite, as well as pre-TSR and post-TSR calcite, has been recognized in the Lower Triassic Feixianguan Formation carbonate reservoir in the Sichuan Basin, China. Pre-TSR calcite has fluid inclusion homogenization temperatures of <110 °C and salinity up to 24 wt.% Post-TSR calcite has fluid inclusion homogenization temperatures of 185 °C down to 120 °C with the lower representing post inversion conditions. Post-TSR calcite has relatively low salinity (as low 4 wt.%).
2. TSR calcite, with carbon isotope values down to −20.2‰ VPDB, has a range of fluid inclusion homogenization temperatures from 115 to >181 °C. TSR calcite has a wide range of fluid inclusion salinity values (5–25 wt.% NaCl). Fluid inclusion salinity decreases with increasing fluid inclusion homogenization temperature.
3. The pre-TSR formation water was progressively diluted by the addition of water created during TSR by the oxidation of hydrogen in alkane gases (including methane) by sulfate. The initial pore water in the gas field, present before TSR, was diluted by the addition of approximately four initial pore water volumes of TSR-created water.
4. Oxygen isotope calculations suggest that water generated by TSR is isotopically lighter than water that would have equilibrated with the bulk rock during burial and heating. The oxygen in the TSR-created water must have originated from the parent anhydrite, with the isotopes partitioned between the product water and product calcite. The TSR-water with the lowest $\delta^{18}O$ is associated with TSR calcite that grew at the highest temperature and thus experienced the most extreme degree of TSR.
5. Water is vital to diagenetic reactions such as TSR itself, as well as the dissolution of carbonate minerals to create secondary pores, reaction of ferroan carbonates with H_2S to create pyrite, etc. The generation of low salinity, low $\delta^{18}O$ water associated with advanced TSR in the Feixianguan Formation, Sichuan Basin, found here, has also been reported in the Permian Khuff Formation in Abu Dhabi (Worden et al., 1996), and from sour Devonian fields in the Western Canada Basin (Yang et al., 2001). This suggests that TSR-derived water may be a common phenomenon, the effects of which have hitherto been underappreciated.

ACKNOWLEDGMENTS

This work has been financially supported by China National Funds for Distinguished Young Scientists (Grant No. 41125009), the Natural Science Foundation of China (Grant Nos. 41402132 and 40839906), and a China Postdoctoral Science Foundation award (Grant No. 2014M550835).

REFERENCES

Alonso-Azcarate J., Bottrell S. H. and Tritlla J. (2001) Sulfur redox reactions and formation of native sulfur veins during low grade metamorphism of gypsum evaporites, Cameros Basin (NE Spain). *Chem. Geol.* **174**, 389–402.

Alonso-Azcarate J., Bottrell S. H. and Mas J. R. (2006) Synsedimentary versus metamorphic control of S, O and Sr isotopic compositions in gypsum evaporites from the Cameros Basin, Spain. *Chem. Geol.* **234**, 46–57.

Archer S. J. and Wall C. G. (1986) *Petroleum Engineering; Principles and Practice*. Graham and Trotman, London.

Bildstein O., Worden R. H. and Brosse E. (2001) Assessment of anhydrite dissolution as the rate-limiting step during thermochemical sulfate reduction. *Chem. Geol.* **176**, 173–189.

Bodnar R. J. (2003) Reequilibration of fluid inclusions. In *Fluid Inclusions—Analysis and Interpretation; Special Publication* (eds. I. Sampson, A. Anderson and D. Marshall). Mineralogical Association of Canada. pp. 213–231.

Boschetti T., Cortecci G., Toscani L. and Iacumin P. (2011) Sulfur and oxygen isotope compositions of Upper Triassic sulfates from northern Apennines (Italy): paleogeographic and hydrogeochemical implications. *Geol. Acta* **9**, 129–147.

Cai C. F., Hu W. S. and Worden R. H. (2001) Thermochemical sulphate reduction in Cambro-Ordovician carbonates in Central Tarim. *Mar. Pet. Geol.* **18**, 729–741.

Cai C. F., Worden R. H., Bottrell S. H., Wang L. S. and Yang C. C. (2003) Thermochemical sulphate reduction and the generation of hydrogen sulphide and thiols (mercaptans) in Triassic carbonate reservoirs from the Sichuan Basin, China. *Chem. Geol.* **202**, 39–57.

Cai C. F., Xie Z. Y., Worden R. H., Hu G. Y., Wang L. S. and He H. (2004) Methane-dominated thermochemical sulphate reduction in the Triassic Feixianguan formation East Sichuan Basin, China: towards prediction of fatal H_2S concentrations. *Mar. Pet. Geol.* **21**, 1265–1279.

Cai C. F., Li K. K., Zhu Y. M., Xiang L., Jiang L., Tenger, Cai X. Y. and Cai L. L. (2010) TSR origin of sulfur in Permian and Triassic reservoir bitumen, East Sichuan Basin, China. *Org. Geochem.* **41**, 871–878.

Cai C. F., Cai L. L., Zhang J., Cai X. Y. and Li K. K. (2012) H_2S-generation by methane-dominated TSR and carbon isotope fractionation in Lower Triassic Feixianguan Formation, Northeast Sichuan Basin. *Acta Petrol. Sinica* **28**, 889–894.

Cai C. F., Zhang C. M., He H. and Tang Y. J. (2013) Carbon isotope fractionation during methane-dominated TSR in East Sichuan Basin gasfields, China: a review. *Mar. Pet. Geol.* **48**, 100–110.

Cai C. F., He W. X., Jiang L., Li K. K., Xiang L. and Jia L. Q. (2014) Petrological and geochemical constraints on porosity difference between Lower Triassic sour- and sweet-gas carbonate reservoirs in the Sichuan Basin. *Mar. Pet. Geol.* **56**, 34–50.

Chafetz H. S., Wu Z., Lapen T. J. and Milliken K. L. (2008) Geochemistry of preserved Permian aragonitic cements in the tepees of the Guadalupe Mountains, West Texas and New Mexico, USA. *J. Sediment. Res.* **78**, 187–198.

Claypool G. E., Holser W. T., Kaplan I. R., Sakai H. and Zak I. (1980) The age curves of sulfur and oxygen isotopes in marine sulfate and their mutual interpretation. *Chem. Geol.* **28**, 199–260.

Du C. G., Hao F. and Huayoa Z. (2007) Effect of thermochemical sulfate reduction upon carbon gas reservoir: an example from the northeast Sichuan basin. *Acta Geol. Sinica – English Edition* **81**, 119–126, in Chinese.

Ehrenberg S. N., Walderhaug O. and Bjorlykke K. (2012) Carbonate porosity creation by mesogenetic dissolution: reality or illusion? *Am. Assoc. Pet. Geol. Bull.* **96**, 217–233.

Friedman I. and O'Neil J. R. (1977) Compilation of stable isotope fractionation factors of geochemical interest. In *Data of Geochemistry*, 6th ed. (ed. M. Fleischer), U.S.G.S. Prof. Surv. Par. 440-KK.

Hao F., Guo T. L., Zhu Y. M., Cai X. Y., Zou H. Y. and Li P. P. (2008) Evidence for multiple stages of oil cracking and thermochemical sulfate reduction in the Puguang gas field, Sichuan Basin, China. *Am. Assoc. Pet. Geol. Bull.* **92**, 611–637.

Hao F., Guo T. L., Du C. G., Zou H. Y., Cai X. Y., Zhu Y. M., Li P. P., Wang C. W. and Zhang Y. C. (2009) Accumulation mechanisms and evolution history of the giant Puguang gas field, Sichuan Basin, China. *Acta Geol. Sinica – English Edition* **83**, 136–145.

Heydari E. (1997) The role of burial diagenesis in hydrocarbon destruction and H_2S accumulation, upper Jurassic Smackover Formation, Black Creek Field, Mississippi. *Am. Assoc. Pet. Geol. Bull.* **81**, 26–45.

Heydari E. and Moore C. H. (1989) Burial diagenesis and thermochemical sulfate reduction, Smackover Formation, southeastern Mississippi salt basin. *Geology* **17**, 1080–1084.

Heydari E., Moore C. H. and Sassen R. (1988) Late burial diagenesis driven by thermal-degradation of hydrocarbons and thermochemical sulfate reduction – Upper Smackover carbonates, southeast Mississippi salt basin. *Am. Assoc. Pet. Geol. Bull.* **72**, 197.

Hosgormez H., Yalcin M. N., Soylu C. and Bahtiyar I. (2014) Origin of the hydrocarbon gases carbon dioxide and hydrogen sulfide in Dodan Field (SE-Turkey). *Mar. Pet. Geol.* **57**, 433–444.

Huang S. J., Huang K. K., Lu J. and Lan Y. F. (2012) Carbon isotopic composition of Early Triassic marine carbonates, Eastern Sichuan Basin, China. *Sci. China-Earth Sci.* **55**, 2026–2038.

Jiang L., Cai C. F., Worden R. H., Li K. K. and Xiang L. (2013) Reflux dolomitization of the Upper Permian Changxing Formation and the Lower Triassic Feixianguan Formation, NE Sichuan Basin, China. *Geofluids* **13**, 232–245.

Jiang L., Worden R. H. and Cai C. F. (2014a) Thermochemical sulfate reduction and fluid evolution of the Lower Triassic Feixianguan Formation sour gas reservoirs, northeast Sichuan Basin, China. *Am. Assoc. Pet. Geol. Bull.* **98**, 947–973.

Jiang L., Worden R. H., Cai C. F., Li K. K., Xiang L., Cai L. L. and He X. Y. (2014b) Dolomitization of gas reservoirs: the Upper Permian Changxing and Lower Triassic Feixianguan Formations, northeast Sichuan Basin, China. *J. Sediment. Res.* **84**, 792–815.

Jiang L., Pan W., Cai C. F., Jia L., Pan L., Wang T., Li H., Chen S. and Chen Y. (2015) Fluid mixing induced by hydrothermal activity in the Ordovician carbonates in Tarim Basin, China. *Geofluids* **15**. http://dx.doi.org/10.1111/gfl.12125 (in press).

Korte C., Jasper T., Kozur H. W. and Veizer J. (2005a) $D^{18}O$ and $d^{13}C$ of Permian brachiopods: a record of seawater evolution and continental glaciation. *Palaeogeogr. Palaeoclimatol. Palaeoecol.* **224**, 333–351.

Korte C., Kozur H. W. and Veizer J. (2005b) $D^{13}C$ and $d^{18}O$ values of Triassic brachiopods and carbonate rocks as proxies for coeval seawater and palaeotemperature. *Palaeogeogr. Palaeoclimatol. Palaeoecol.* **226**, 287–306.

Krouse H. R., Viau C. A., Eliuk L. S., Ueda A. and Halas S. (1988) Chemical and isotopic evidence of thermochemical sulfate reduction by light hydrocarbon gases in deep carbonate reservoirs. *Nature* **333**, 415–419.

Li K. K., Cai C. F., Jiang L., Cai L. L., Jia L. Q., Zhang B., Xiang L. and Yuan Y. Y. (2012) Sr evolution in the Upper Permian and Lower Triassic carbonates, northeast Sichuan basin, China: constraints from chemistry, isotope and fluid inclusions. *Appl. Geochem.* **27**, 2409–2424.

Liu Q. Y., Worden R. H., Jin Z. J., Liu W. H., Li J., Gao B., Zhang D. W., Hu A. P. and Yang C. (2013) TSR versus non-TSR processes and their impact on gas geochemistry and carbon stable isotopes in Carboniferous, Permian and Lower Triassic marine carbonate gas reservoirs in the Eastern Sichuan Basin, China. *Geochim. Cosmochim. Acta* **100**, 96–115.

Liu Q. Y., Worden R. H., Jin Z. J., Liu W. H., Li J., Gao B., Zhang D. W., Hu A. P. and Yang C. (2014) Thermochemical sulphate reduction (TSR) versus maturation and their effects on hydrogen stable isotopes of very dry alkane gases. *Geochim. Cosmochim. Acta* **137**, 208–220.

Ma Y. S. (2008) Geochemical characteristics and origin of natural gases from Puguang gas field on Eastern Sichuan Basin. *Nat. Gas Geosci.* **19**, 1–7 (in Chinese).

Ma Y. S., Zhang S. C., Guo T. L., Zhu G. Y., Cai X. Y. and Li M. W. (2008) Petroleum geology of the Puguang sour gas field in the Sichuan Basin, SW China. *Mar. Pet. Geol.* **25**, 357–370.

Machel H. G. (1987) Saddle dolomite as a by-product of chemical compaction and thermochemical sulfate reduction. *Geology* **15**, 936–940.

Machel H. G. (1998) Comment on "The effects of thermochemical sulfate reduction upon formation water salinity and oxygen isotopes in carbonate reservoirs". *Geochim. Cosmochim. Acta* **62**, 337–341.

Machel H. G. (2001) Bacterial and thermochemical sulfate reduction in diagenetic settings – old and new insights. *Sed. Geol.* **140**, 143–175.

Machel H. G., Krouse H. R., Riciputi L. R. and Cole D. R. (1995) Devonian Nisku sour gas play, Canada: a unique natural laboratory for study of thermochemical sulfate reduction. In *Geochemical Transformations of Sedimentary Sulfur* (eds. M. A. Vairavamurthy and M. A. A. Schoonen). pp. 439–454.

Mankiewicz P. J., Pottorf R. J., Kozar M. G. and Vrolijk P. (2009) Gas geochemistry of the Mobile Bay Jurassic Norphlet

Formation: thermal controls and implications for reservoir connectivity. *Am. Assoc. Pet. Geol. Bull.* **93**, 1319–1346.

Manzano B. K., Fowler M. G. and Machel H. G. (1997) The influence of thermochemical sulphate reduction on hydrocarbon composition in Nisku reservoirs, Brazeau river area, Alberta, Canada. *Org. Geochem.* **27**, 507–521.

Ni Y. Y., Liao F. R., Dai J. X., Zou C. N., Zhu G. Y., Zhang B. and Liu Q. Y. (2012) Using carbon and hydrogen isotopes to quantify gas maturity, formation temperature, and formation age – specific applications for gas fields from the Tarim Basin, China. *Energy Explor. Exploit.* **30**, 273–293.

Oakes C. S., Bodnar R. J. and Simonson J. M. (1990) The system NaCl–$CaCl_2$–H_2O: I. The ice liquidus at 1 atm total pressure. *Geochim. Cosmochim. Acta* **54**, 603–611.

Orr W. L. (1977) Geologic and geochemical controls on the distribution of hydrogen sulfide in natural gas. In *Adv. Org. Geochem.* (eds. R. Campos and J. Goni). Enadisma, Madrid, pp. 571–597.

Sassen R. and Moore C. H. (1988) Framework of hydrocarbon generation and destruction in eastern Smackover Trend. *Am. Assoc. Pet. Geol. Bull.* **72**, 649–663.

Sassen R., Snelling R. D. and Heydari E. (1991) Destruction of hydrocarbons and generation of nonhydrocarbon gases in deep carbonate reservoirs of the Smackover Formation. *Org. Geochem.* **17**, 273.

Vandeginste V., Swennen R., Gleeson S. A., Ellam R. M., Osadetz K. and Roure F. (2009) Thermochemical sulphate reduction in the Upper Devonian Cairn Formation of the Fairholme carbonate complex (South-West Alberta, Canadian Rockies): evidence from fluid inclusions and isotopic data. *Sedimentology* **56**, 439–460.

Veizer J., Ala D., Azmy K., Bruckschen P., Buhl D., Bruhn F., Carden G. A. F., Diener A., Ebneth S., Godderis Y., Jasper T., Korte C., Pawellek F., Podlaha O. G. and Strauss H. (1999) Sr-87/Sr-86, delta C-13 and delta O-18 evolution of Phanerozoic seawater. *Chem. Geol.* **161**, 59–88.

Videtich P. E. (1994) Dolomitization and H_2S generation in the Permian Khuff Formation, offshore Dubai, UAE. *Carbonates Evaporites* **9**, 42–57.

Vinogradov V. I., Belenitskaya G. A., Bujakaite M. I., Kuleshov V. N., Minaeva M. A. and Pokrovskii B. G. (2006a) Isotopic signatures of deposition and transformation of Lower Cambrian saliferous rocks in the Irkutsk amphitheater: Communication 1. Sulfur isotopic composition. *Lithol. Min. Resour.* **41**, 85–97.

Vinogradov V. I., Belenitskaya G. A., Bujakaite M. I., Kuleshov V. N., Minaeva M. A. and Pokrovskii B. G. (2006b) Isotopic signatures of deposition and transformation of Lower Cambrian saliferous rocks in the Irkutsk Amphitheater: Communication 3. Carbon and oxygen isotopic compositions in carbonates. *Lithol. Min. Resour.* **41**, 271–279.

Wang Y. M., Dou L. R., Wen Y. C., Zhang J. Y. and Jiu H. Y. (2002) Origin of Triassic Feixianguan Formation gas pools in Northeastern Sichuan Basin, China. *Geochimica* **21**, 517–524 (in Chinese).

Wang Y. G., Wen Y. C. and Hong H. T. (2007) Diagenesis of Triassic Feixianguan Formation in Sichuan basin, southwest China. *Acta Sedimentol. Sin.* **25**, 831–839 (in Chinese).

Worden R. H. and Smalley P. C. (1996) H_2S-producing reactions in deep carbonate gas reservoirs: Khuff Formation, Abu Dhabi. *Chem. Geol.* **133**, 157–171.

Worden R. H. and Smalley P. C. (2004) Does methane react during thermochemical sulphate reduction? Proof from the Khuff Formation, Abu Dhabi. In *Water–Rock Interaction* (eds. R. Wanty and R. R. Seal). Taylor and Francis Group, London, pp. 1049–1053.

Worden R. H., Smalley P. C. and Oxtoby N. H. (1995) Gas souring by thermochemical sulfate reduction at 140 °C. *Am. Assoc. Pet. Geol. Bull.* **79**, 854–863.

Worden R. H., Smalley P. C. and Oxtoby N. H. (1996) The effects of thermochemical sulfate reduction upon formation water salinity and oxygen isotopes in carbonate gas reservoirs. *Geochim. Cosmochim. Acta* **60**, 3925–3931.

Worden R. H., Smalley P. C. and Oxtoby N. H. (1998) Reply to the comment by H.G. Machel on "The effects of thermochemical sulfate reduction upon formation water salinity and oxygen isotopes in carbonate reservoirs". *Geochim. Cosmochim. Acta* **62**, 343–346.

Worden R. H., Smalley P. C. and Cross M. M. (2000) The influence of rock fabric and mineralogy on thermochemical sulfate reduction: Khuff Formation, Abu Dhabi. *J. Sediment. Res.* **70**, 1210–1221.

Yang C., Hutcheon I. and Krouse H. R. (2001) Fluid inclusion and stable isotopic studies of thermochemical sulphate reduction from Burnt Timber and Crossfield East gas fields in Alberta, Canada. *Bull. Can. Pet. Geol.* **49**, 149–164.

Zhao W. Z., Luo P., Chen G. S., Cao H. and Zhang B. M. (2005) Origin and reservoir rock characteristics of dolostones in the Early Triassic Feixianguan Formation, NE Sichuan Basin, China: significance for future gas exploration. *J. Pet. Geol* **28**, 83–100.

Zhao W. Z., Xu C. C., Wang T. S., Wang H. J., Wang Z. C., Bian C. S. and Li X. (2011) Comparative study of gas accumulations in the Permian Changxing reefs and Triassic Feixianguan oolitic reservoirs between Longgang and Luojiazhai-Puguang in the Sichuan Basin. *Chin. Sci. Bull.* **56**, 3310–3320.

Zhu G. Y., Zhang S. C., Liang Y. B., Dai J. X. and Li J. (2005a) Isotopic evidence of TSR origin for natural gas bearing high H_2S contents within the Feixianguan Formation of the north-eastern Sichuan Basin, southwestern China. *Sci. China Series D-Earth Sci.* **48**, 1960–1971.

Zhu G. Y., Zhang S. C., Liang Y. B., Dai J. X. and Li J. (2005b) Origins of high H_2S-bearing natural gas in China. *Acta Geol. Sinica-English Edition* **79**, 697–708.

Zhu G. Y., Zhang S. C., Liang Y. B., Zhou G. Y. and Wang Z. J. (2007) Formation mechanism and controlling factors of natural gas reservoirs of the Jialingjiang formation in the east Sichuan Basin. *Acta Geol. Sinica-English Edition* **81**, 805–816.

Associate editor: Jack J. Middelburg